

# **THE USE OF TRANSFINITE ELEMENTS IN THE METHODS OF MOMENTS APPLIED TO ELECTROMAGNETIC SCATTERING BY DIELECTRIC CYLINDERS**

Ph. De Doncker

Université Libre de Bruxelles  
Av Roosevelt 50  
CP 165/51 Elecgen  
1050 Bruxelles, Belgium

- 1. Introduction**
  - 2. The Transfinite Elements**
    - 2.1 The Transfinite Interpolation
    - 2.2 The Geometrical Modeling
    - 2.3 The Interpolation Process
  - 3. The Results**
    - 3.1 Convergence Rates of the Internal Field
    - 3.2 Stability of the VSIE
    - 3.3 Choice of a Discretization Method
  - 4. Conclusion**
- Appendix**  
**References**

## **1. INTRODUCTION**

The electromagnetic scattering by dielectric bodies is an important problem in many applications, namely in the study of the interactions of waves with biological tissues. These studies have received much attention in the last few years due to the rapid growing of the mobile communication devices on one hand and of the medical devices on the other hand. Most often, they utilize two numerical methods: the Finite Difference Time Domain method [1] and the Method of Moments (MoM) [2] applied to surface or volume integral equations. This last

method has the advantage to automatically incorporate the Sommerfeld radiation condition. However there has been a lot of discussions about the reliability of its results [3]. As we will see, even in the two-dimensional case, the MoM seems to present inaccuracies or instabilities when applied to the wave scattering by dielectric cylinders in the TE case (electric field transverse to the axis of the cylinder). Moreover, only a few works deal with the systematic study of the improvements of the stability or of the convergence rate of the MoM in such cases surely owing to the erratic behavior of the solutions. Our goal is to fill in this gap introducing a general theory to study separately the effects of the geometrical description and of the interpolation schemes in the MoM: the transfinite elements theory. Although we aim at using it to use this theory in three-dimensional problems, we restricted ourselves here to the two-dimensional case on one hand to decrease the computational complexity to validate the new formulation and on the other hand because till now, such a study has not been carried out in two dimensions where a lot of questions remain unanswered.

The original formulation of the electromagnetic scattering by dielectric cylinders is due to Richmond [4, 5]. His work is based on an Electric Field Integral Equation (EFIE) in both the TM and TE cases and used the point matching method in combination with a pulse approximation of the unknown field on square cells dividing the cylinder cross-section. Due to the structure of the matrix obtained with the Richmond's formulation, Borup et al. extended this work using the FFT algorithm to reduce the computational needs [6]. However, they pointed out some problems occurring with the EFIE in the TE case. They found that the accuracy of the method can become problematic if square cells are used because of the rough description of the air-dielectric interface at the boundary of the cylinder. They also found that in the TE case the discontinuities of the electric field due to the pulse approximation leads to the presence of spurious line charges which dramatically decrease the accuracy of the solution. They concluded that to ensure the stability and accuracy of the Richmond's formulation, quadrilateral cells and linear interpolation must be used in place of the square cells and the pulse interpolation of the original work.

The problems encountered in [6] can be partially avoided by using a Magnetic Field Integral Equation (MFIE) in the TE case in place of the EFIE. Peterson and Klock [7] have developed a MFIE where the magnetic field is linearly interpolated on triangular cells. Jin et al. have

proposed [10] a Volume-Surface Integral Equation (VSIE) which presents in a unified formalism a scalar integral equation for both the TM and TE cases (an EFIE in the TM case and a MFIE in the TE case). They applied this method in combination with the quadratic isoparametric elements often encountered in the finite element methods [8]. These two formulations are stable and accurate in all cases but none of the authors presents a systematic study of the effects of the geometrical description and of the interpolation schemes.

To our knowledge, a comparison of the convergence rates of all the different interpolation schemes or a comparison of the different geometrical modelings does not appear in the literature although it seems to be a very important study for the optimal choice of a method. For example, in [8], we could think of using quadrilateral or square cells in place of the more complex parabolic ones. It would be very important to answer to this question because in applications such as in biomedical engineering the use of simple discretization grids could be preferable to simplify the very difficult mesh generation task. Moreover, to be competitive with respect to differential equations based numerical methods, the MoM must be compatible with iterative solvers optimized by the FFT algorithm for the matrix — vector products calculations and it is the case only when a regular discretization grid is used. To try to answer to these questions, we developed a VSIE based MoM employing transfinite elements which are a generalization of all the elements appearing in the literature.

The transfinite elements theory is a tool originally developed for the geometrical problems of computer-aided design (CAD). It has been rapidly adapted to the problem of curvilinear mesh generation for finite element analysis [9] and it is now become a standard method for surface and volume modeling [14]. Most of its applications are based on its geometrical features. However, the transfinite elements also present special properties from the interpolation theory point of view which are more barely known. Our MoM formulation makes use of the combination of the geometrical and interpolational features of the transfinite elements.

## 2. THE TRANSFINITE ELEMENTS

### 2.1 The Transfinite Interpolation

Both the geometrical modeling and the interpolation process of the MoM can be formulated thanks to the transfinite interpolation theory which will be briefly outlined here in the two-dimensional case. For a further reading see [9].

To construct an interpolant of a function  $\phi(s, t)$  on a region  $\mathfrak{S} : [0, h] \times [0, h]$ , let the one-dimensional interpolation projectors  $P_s$  and  $P_t$  be defined as

$$\begin{aligned} P_s \phi(s, t) &= \sum_{m=1}^M \phi(s_m, t) u_m(s) \\ P_t \phi(s, t) &= \sum_{n=1}^N \phi(s, t_n) v_n(t) \end{aligned} \quad (1)$$

where  $s_m$  and  $t_n$  are two sets of interpolation nodes  $\in \mathfrak{S}$  and  $\{u_m(s)\}$  and  $\{v_n(t)\}$  are the associated interpolation basis functions which are non-zero only over  $\mathfrak{S}$ . If those functions satisfy the cardinality condition

$$\begin{aligned} u_m(s_l) &= \delta_{ml} \\ v_n(t_l) &= \delta_{nl} \end{aligned} \quad (2)$$

it is easy to see that  $P_s$  and  $P_t$  are two commutative projectors (i.e., two commutative linear idempotent operators). To obtain a two-dimensional interpolant of  $\phi(s, t)$  on  $\mathfrak{S}$  it is necessary to blend the two projections defined by (1). In the classical interpolation theory, the two-dimensional interpolant  $\tilde{\phi}(s, t)$  of  $\phi(s, t)$  is given by the *tensor-product* projection

$$\tilde{\phi}(s, t) = P_s P_t \phi(s, t) \quad (3)$$

It is easy to see that the accuracy set of this projection (defined as the set of points where the interpolant  $\tilde{\phi}$  equals the original function  $\phi$ ) is formed by the nodes  $(s_m, t_n)$

$$\tilde{\phi}(s_m, t_n) = \phi(s_m, t_n) \quad (4)$$

On the other hand we can consider another approximation  $\pi(s, t)$  of  $\phi(s, t)$  obtained by application of the *boolean sum* projection:

$$\pi(s, t) = (P_s \oplus P_t) \phi(s, t) \quad (5)$$

where the boolean sum of two commutative projectors  $A$ ,  $B$  is defined as

$$(A \oplus B)\phi = (B \oplus A)\phi = (A + B - AB)\phi \quad (6)$$

It is possible to show that the accuracy set of  $\pi(s, t)$  is formed by the lines  $(s_m, t)$ ,  $(s, t_n)$  and it thus consists of an infinite number of points whence the name of transfinite interpolant, of  $\phi(s, t)$ . This special property is the starting point of the application of the transfinite interpolation in the geometrical modeling and in the interpolation process in the MoM.

### 2.2 The Geometrical Modeling

In the MoM analysis of the electromagnetic scattering by a non-homogeneous dielectric cylinder, the first step is to divide the cross-section  $S$  of the cylinder in small elements generally called patches or cells. The conventional two-dimensional MoM involves the partitioning of  $S$  in rectangular or triangular elements. As it will be shown further, when  $S$  is a non-polygonal domain, such a polygonal approximation could become a serious problem for the stability and the convergence of the method. To circumvent this problem, Jin et al. have developed a MoM employing isoparametric quadratic elements whose sides are parabolic segments. Thanks to the transfinite interpolation theory, it is possible to extend this class of cells to elements whose sides are described by arbitrary curved segments.

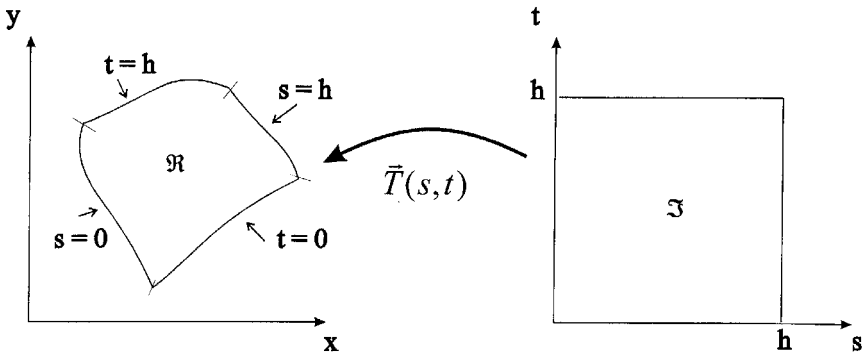


Figure 1. The  $\mathcal{R}$  and  $\mathcal{S}$  domains.

Let  $\mathfrak{R}$  be a closed, bounded and simply connected domain in the physical  $xy$ -plane whose boundary  $\partial\mathfrak{R}$  is subdivided into four parametric curved segments. To construct a curvilinear coordinate system on  $\mathfrak{R}$  let

$$\vec{T}(s, t) = \begin{pmatrix} x(s, t) \\ y(s, t) \end{pmatrix} \quad (7)$$

be an univalent mapping of the square  $\mathfrak{S} : [0, h] \times [0, h]$  in the  $(s, t)$  parameters plane onto  $\mathfrak{R}$  in the  $xy$ -plane (see Fig. 1) i.e.  $\vec{T} : \mathfrak{S} \rightarrow \mathfrak{R}$  provides a unique correspondence between a point  $(s, t) \in \mathfrak{S}$  and its image  $(x(s, t), y(s, t)) \in \mathfrak{R}$ . If  $\vec{F}(0, t)$ ,  $\vec{F}(h, t)$ ,  $\vec{F}(s, 0)$ ,  $\vec{F}(s, h)$  are the four compatible parametric curves describing  $\partial\mathfrak{R}$ , and if  $P_s$ ,  $P_t$  are two projectors on linear Lagrange basis functions,  $\vec{T}(s, t)$  is given in the transfinite elements theory by [9]:

$$\begin{aligned} \vec{T}(s, t) &= (P_s \oplus P_t) \vec{F}(s, t) \\ &= \frac{h-s}{h} \vec{F}(0, t) + \frac{s}{h} \vec{F}(h, t) + \frac{h-t}{h} \vec{F}(s, 0) \\ &\quad + \frac{t}{h} \vec{F}(s, h) - \frac{(h-s)(h-t)}{h^2} \vec{F}(0, 0) - \frac{st}{h^2} \vec{F}(h, h) \\ &\quad - \frac{(h-t)s}{h^2} \vec{F}(h, 0) - \frac{(h-s)t}{h^2} \vec{F}(0, h) \end{aligned} \quad (8)$$

It is easy to see that the image in the  $xy$ -plane of the lines  $s = \text{constant}$  and  $t = \text{constant}$  draws a curvilinear mesh in  $\mathfrak{R}$  formed by a set of what is called transfinite elements and that any function  $f(x, y)$  defined on  $\mathfrak{R}$  corresponds to a function  $f^*(s, t)$  defined on  $\mathfrak{S}$  by the identification:

$$f(x(s, t), y(s, t)) = f^*(s, t) \quad (s, t) \in \mathfrak{S} \quad (9)$$

When dealing with the description of the cross-section of a cylinder in the MoM, transformations like  $\vec{T}(s, t)$  can be applied once for the whole cross-section, several times for different parts of it or even separately for each cell dividing the cross-section (the inner mesh is of course in this case not necessary). It is important to note that thanks to the properties of the transfinite interpolation, if the shape of the cylinder is analytically known, the transfinite mesh exactly matches the cross-section without any approximation. Otherwise, the four functions  $\vec{F}(0, t)$ ,  $\vec{F}(h, t)$ ,  $\vec{F}(s, 0)$ ,  $\vec{F}(s, h)$  can represent approximations by piecewise linear or quadratic functions of the real cross-section shape

and  $\vec{T}(s, t)$  is in this case equivalent to a meshing by respectively quadrilateral (or triangular) and parabolic elements. All the meshes encountered in the conventional MoM can thus be generated thanks to the transfinite elements. Fig. 2 gives two examples of transfinite meshes (for other examples or some generalizations see [9]).

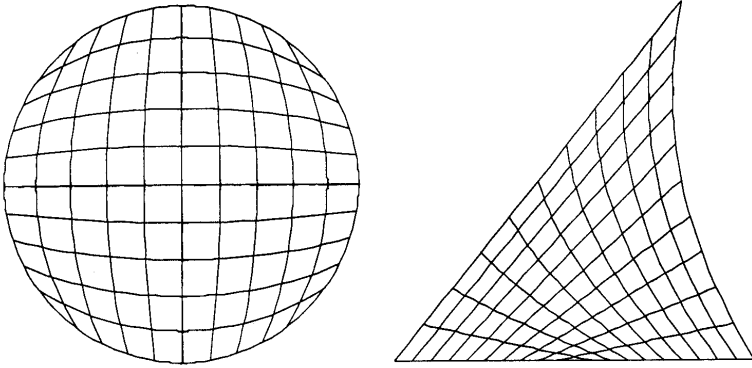


**Figure 2.** Examples of transfinite meshes.

If  $f(x, y)$  is an unknown scalar field appearing in an integral equation, its corresponding transform  $f^*(s, t)$  can directly be interpolated over each element in the curvilinear coordinate system  $(s, t)$  defined by (8). When an interpolation scheme is used in combination with a transfinite mesh which exactly matches the boundary of the cylinder, the solution obtained is the best which can be reached with any other simpler cells (quadrilateral, parabolic, ...) The transfinite elements theory hence provides a reference solution to evaluate the accuracy of a method and allows an easy separate study of the effects of the geometrical description and of the interpolation schemes.

### 2.3 The Interpolation Process

Let  $\phi(s, t)$  be the unknown function appearing in the MoM (and which could eventually represents a component of a vectorial field). The transfinite interpolant (5) of  $\phi(s, t)$  over a cell  $\mathfrak{S} : [0, h] \times [0, h]$  in the  $st$ -plane can be explicitly written

$$\pi(s, t) = (P_s + P_t - P_s P_t)\phi(s, t) \quad (10)$$

Of course, to obtain an algebraic system, only points values of  $\phi(s, t)$  can appear in the interpolant and a *second level interpolation* is necessary for the terms  $P_s\phi$  and  $P_t\phi$ . This results in a new interpolant  $\tilde{\pi}(s, t)$  of  $\phi(s, t)$ :

$$\tilde{\pi}(s, t) = (P_s \tilde{P}_t + \tilde{P}_s P_t - P_s P_t)\phi(s, t) \quad (11)$$

where  $\tilde{P}_s$  and  $\tilde{P}_t$  are second level interpolation projectors.

In this general formalism, the classical interpolation schemes are obtained if  $\tilde{P}_s = P_s$  and  $\tilde{P}_t = P_t$  so that (11) becomes the classical tensor product interpolation  $P_s P_t \phi(s, t)$ . For a two-dimensional pulse approximation,  $P_s$  and  $P_t$  are chosen as projectors on piecewise constant basis functions in the  $st$ -plane and considering the supremum norm  $\|\cdot\|$  defined on the interpolation cell of sides  $h$ , asymptotically when  $h \rightarrow 0$ , the interpolation error can be shown to be  $\varepsilon \sim \mathcal{O}(h)$  [12]. For a classical linear (rooftop) interpolation,  $P_s$ ,  $P_t$ ,  $\tilde{P}_s$  and  $\tilde{P}_t$  are chosen to be projectors on a linear Lagrange interpolation basis:

$$\begin{aligned} P_s \phi(s, t) &= \tilde{P}_s \phi(s, t) = \frac{h-s}{h} \phi(0, t) + \frac{s}{h} \phi(h, t) \\ P_t \phi(s, t) &= \tilde{P}_t \phi(s, t) = \frac{h-t}{h} \phi(s, 0) + \frac{t}{h} \phi(s, h) \end{aligned} \quad (12)$$

and the interpolation error is  $\varepsilon \sim \mathcal{O}(h^2)$ .

But the transfinite interpolation theory shows that it is possible to enhance the accuracy of the projection keeping the same first level projectors  $P_s$ ,  $P_t$  but taking  $\tilde{P}_s$  and  $\tilde{P}_t$  as univariate projectors on a quadratic Lagrange basis:

$$\begin{aligned} \tilde{P}_s \phi(s, t) &= \frac{(s-h/2)(s-h)}{h^2/2} \phi(0, t) + \frac{s(h-s)}{h^2/4} \phi(h/2, t) \\ &\quad + \frac{s(s-h/2)}{h^2/2} \phi(h, t) \end{aligned}$$



$$\begin{aligned} \tilde{P}_t\phi(s, t) = & \frac{(t - h/2)(t - h)}{h^2/2}\phi(s, 0) + \frac{t(h - t)}{h^2/4}\phi(s, h/2) \\ & + \frac{t(t - h/2)}{h^2/2}\phi(s, h) \end{aligned} \quad (13)$$

It is possible to show [12] that in this case the interpolation error is  $\varepsilon \sim \mathcal{O}(h^3)$  and that the eight interpolation nodes are located on the boundary of the cell (see Fig. 4(c)). This interpolation is in fact a generalization of the isoparametric interpolation used in [8]. It is still possible to enhance the accuracy of the interpolation by taking a second level cubic projection to reach the optimal error in the case of a first level linear projection ( $\varepsilon \sim \mathcal{O}(h^4)$ ). But the transfinite quadratic interpolation appears as a good trade-off between accuracy and numerical complexity and cubic interpolation will not be considered here.

Thanks to the projectors formalism it is easy to generalize the geometrical modeling and the interpolation process to three dimensions as it is shown in the appendix.

### 3. THE RESULTS

In this work, we compared three different kinds of cells (see Fig. 3): the square cells, the quadrilateral cells and the transfinite cells which provide the reference solutions. Each of those cells were used in combination with three interpolation schemes: the pulse interpolation (one interpolation node per cell), the linear interpolation (four nodes per cell) and the transfinite quadratic interpolation (eight nodes per cell). The interpolation nodes corresponding to an arbitrary curved cell are shown on Fig. 4.

To construct the transfinite mesh on the cross-section of the cylinder we considered the transformation by  $\vec{T}(s, t)$  of a square  $[0, 1] \times [0, 1]$  in the  $st$ -plane meshed by square cells of size  $h$ . To construct a quadrilateral mesh, we considered a transformation of this same square mesh by a piecewise linear approximation of  $\vec{T}(s, t)$ .

When dealing with the interaction of electromagnetic waves with dielectric bodies, we are interested in determining both the scattered field and the induced field inside the dielectric. The goal of our work was to indicate which are the respective influences of the geometrical modeling and of the interpolation schemes in the stability and accuracy of the MoM applied to those problems. The Volume-Surface Integral

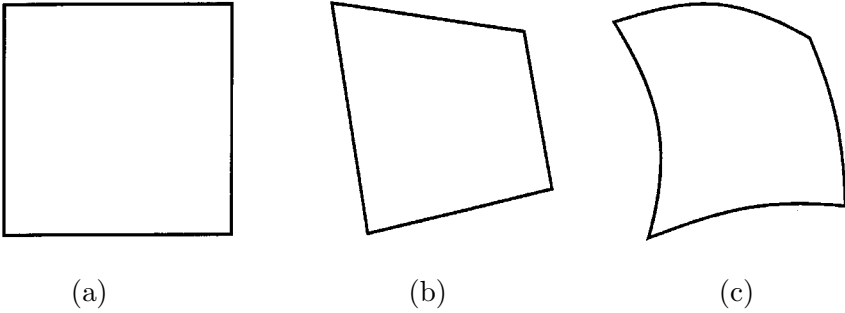


**Figure 3.** The square, quadrilateral and transfinite interpolation cells.

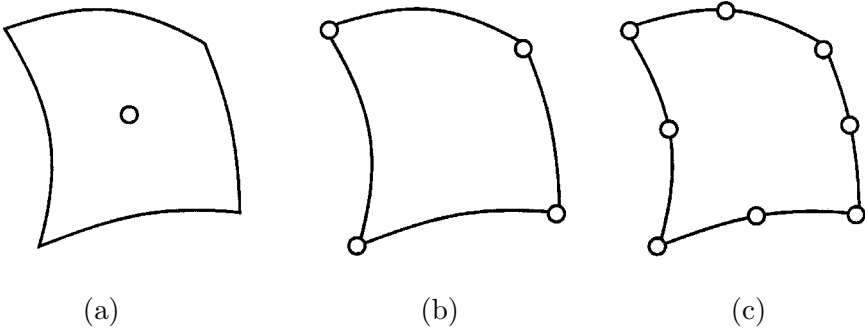


**Figure 4.** Interpolation nodes. (a) Pulse interpolation (b) Linear interpolation (c) Quadratic interpolation.

Equation (VSIE) developed by Jin et al. [8] was chosen to solve the problem because it presents in a unified formalism an integral equation for both the TM and the TE cases and because of its apparent good behavior for any value of the permittivity. We applied with success the VSIE in the transfinite interpolation formalism in the more general inhomogeneous case [13] but we present here solutions to simple academic problems whose analytical solutions are known for an easy interpretation of the results. We first studied the convergence rate of the internal field with the various interpolations schemes. In this case, transfinite elements were used to eliminate the influence of the geometrical modeling. Then, we studied the stability of the calculation of the internal field and of the radar cross section (RCS) with the different cell shapes and the different interpolations. All our numerical results were obtained using the point-matching method to discretize the integral equations.

### 3.1 Convergence Rates of the Internal Field

The convergence rates of the pulse, linear and transfinite quadratic interpolations schemes have been obtained in the TM and TE cases for the problem of the scattering of a plane wave incident on an homogeneous circular cylinder. The error considered to calculate the convergence rates is the r.m.s. error  $\varepsilon$  of the electric field (in the TM case) or of the magnetic field (in the TE case) inside the cylinder defined by

$$\varepsilon = \frac{\sqrt{\iint_S |F_n(\vec{r}) - F_a(\vec{r})|^2 dS}}{\sqrt{\iint_S |F_a(\vec{r})|^2 dS}} \quad (14)$$

where  $F$  represents the electric (in the TM case) or magnetic field (in the TE case),  $F_n$  is the numerical result and  $F_a$  is the analytical one. It is noteworthy that by using the transfinite elements there is absolutely no geometrical approximation neither in the discretization of the integral equation, nor in the calculation of the error. The interpolation scheme is the only numerical parameter which can influence the convergence rates. Fig. 5 shows a typical result in the TM case where the error  $\varepsilon$  is plotted as a function of the cell size  $h$  (cell size in the  $st$ -plane in the cases of the transfinite and the quadrilateral meshes and cell size in the  $xy$ -plane normalized by the cylinder diameter in the square mesh case). Several conclusions can be drawn from this study. The difference of the convergence rates between the pulse and the linear interpolations and between the linear and the quadratic interpolations are of one order of magnitude as predicted by the theory. However, the absolute values of these convergence rates vary with the value of the permittivity and become smaller when the cylinder is close to one of its resonance frequency. As the convergence rate of the quadratic interpolation is higher than the one of the other interpolations, the interpolation nodes density (and hence the total number of unknowns) necessary to obtain a given accuracy is much smaller. Table 1 shows the number of unknowns necessary to obtain a 5% r.m.s. error in the case of a TM or TE plane wave incident on an homogeneous circular dielectric cylinder. The transfinite quadratic interpolation provides a powerful tool to decrease the computational needs and must be preferred to the other schemes if the scatterer is large compared to the free-space wavelength  $\lambda_0$ . Thanks to this interpolation scheme, it is possible to solve problems which would be intractable with the other interpolations.

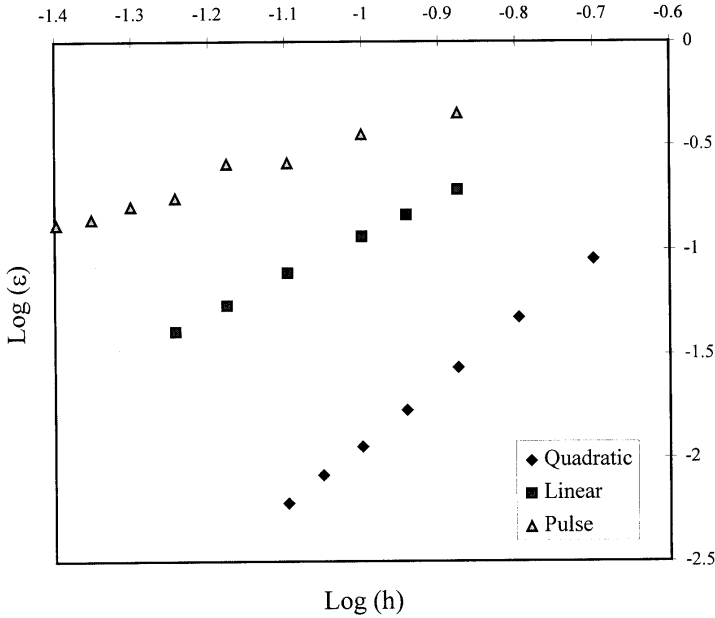


**Figure 5.** r.m.s. error of the electric field for the pulse, linear and quadratic interpolations (TM wave, radius =  $0.1\lambda_0$ ,  $\mu_r = 1$ ,  $\varepsilon_r = 54 - j84$ ).

	radius/ $\lambda_0$	$\varepsilon_r$	Pulse*	Linear	Quadratic
TM	0.4	4	4624	1156	133
	0.1	54-j 84	3844	196	96
TE	0.35	4	5184	625	96
	0.2	54-j 84	44100	1681	481

**Table 1.** Number of unknowns necessary to obtain a 5% r.m.s. error for the different interpolation schemes (plane wave incident on an homogeneous dielectric circular cylinder ( $\mu_r = 1$ ), \* = extrapolated values).

In the TE case, it was problematic to keep a satisfying convergence rate of the internal field because of the difficulty to calculate accurately the matrix elements in the discretization process. In fact, in the VSIE

formulation of the TE case, the factor  $1/\varepsilon_r$  acts as an error amplifier as was already explained in [8]. It is thus very difficult to solve for the TE case for permittivities encountered in biological tissues and the use of a quadratic interpolation is absolutely necessary to keep a sufficiently high convergence rate.

### 3.2 Stability of the VSIE

Two problems have been studied concerning the stability of the VSIE: the computation of the RCS and the computation of the internal field. To compare the numerical results with analytical values, the problem of the plane wave scattering by an homogeneous dielectric circular cylinder was chosen. The three interpolation schemes were employed in combination with the three kinds of cells (square, quadrilateral and transfinite cells).

The main conclusion of our simulations is that no instabilities were found for large values of the relative permittivity  $\varepsilon_r$  neither in the TM nor in the TE case. The VSIE seems thus intrinsically more stable than the EFIE and must be preferred to this latter.

For values of the relative permittivity close to the real axis, the computation of the RCS can be sensitive to the geometrical description of the cylinder. Fig. 6 shows the convergence of the backscatter RCS for the different kinds of elements in combination with the quadratic interpolation (the same kind of results were obtained with the other interpolations). It is easy to see that the convergence when square elements are used is very oscillatory. It can even totally disappears when the cylinder is close to one of its resonance frequency where the value of the RCS very quickly varies with the radius of the cylinder. The numerical results have shown that the three interpolations exhibit rather the same behavior concerning the stability. An improvement of the interpolation alone is thus not sufficient to change the stability of the method. On the other hand, the results obtained with quadrilateral elements are perfectly stable in every cases and their numerical values are very close to the reference values obtained with transfinite elements. The square elements are unpredictable to calculate the RCS but it seems unnecessary to use parabolic elements as in [8].

The computation of the internal field was found to be potentially sensitive to the geometrical description of the cylinder but quadrilateral elements are also sufficient to ensure the stability. The convergence curves for the different cells present the same behavior as the conver-

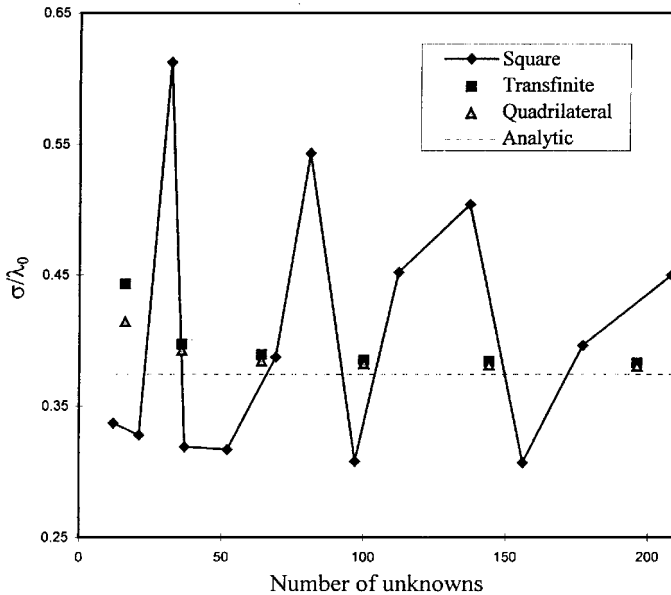


**Figure 6.** Convergence of the normalized backscatter RCS  $\sigma/\lambda_0$  (TM wave, radius =  $0.44\lambda_0$ ,  $\mu_r = 1$ ,  $\varepsilon_r = 4$ ).

gence curves of the RCS. The instability with square elements occurs only close to the resonances of the cylinder and not for biological values of the permittivities as in [6] with the EFIE. Fig. 7 shows a typical example of convergence for the different cells in combination with the pulse interpolation in the case of a large value of  $\varepsilon_r$  (on this figure, the r.m.s. error was calculated along a diameter of the cylinder parallel to the propagation direction of the incident field). Moreover the accuracy obtained with quadrilateral elements and transfinite elements in combination with any interpolation scheme is almost the same.

### 3.3 Choice of a Discretization Method

It is now possible to define which is the best combination of cell shape and interpolation scheme to be used in a VSIE based MoM. As the large numbers of unknowns necessary to obtain accurate results is still the most prohibitive problem of the MoM, it is obvious from the convergence rates study that the transfinite quadratic interpolation must be used in place of the pulse or linear (rooftop) interpolations generally encountered in the literature.

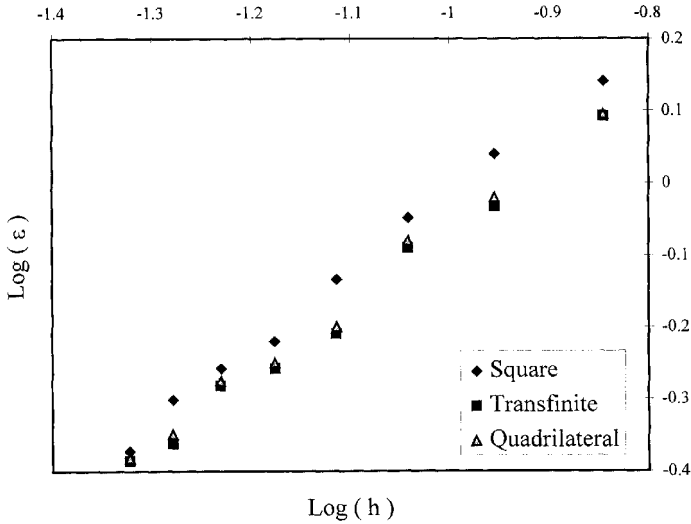


**Figure 7.** r.m.s error of the internal field for the square, quadrilateral and transfinite cells in combination with the pulse interpolation (TE wave, radius =  $0.1\lambda_0$ ,  $\mu_r = 1$ ,  $\varepsilon_r = 72 - j162$ ).

From the stability point of view, the VSIE is stable except near the resonances of the cylinder. In most of the cases, it has been shown that the quadrilateral cells are sufficient to ensure the stability and that the accuracy of the solutions obtained with this kind of cells is very close to the accuracy of the reference solution obtained with the transfinite mesh.

We can thus conclude that when dealing with the problem of the scattering by dielectric cylinders, the best element of our study is a quadrilateral cell used in combination with a quadratic interpolation, i.e., a subparametric element as encountered in the finite element method [11]. However, for high values of the relative permittivity as it is the case in biological tissues, square cells are sufficient to ensure the stability. This fact is important because if a regular square grid is used, all the interpolation functions presented here are invariant to a shift from one cell to another. The matrix of the discretized problem can thus be shown to be block Toeplitz and iterative solvers optimized by the FFT algorithm for the matrix-vector products calculations can be used to solve the algebraic system [15]. This is a condition the MoM has to satisfy to be competitive with respect to the differential equations based methods.

#### 4. CONCLUSION

In order to study the stability and the accuracy of the MoM applied to the scattering by dielectric cylinders, a VSIE based MoM employing transfinite elements was developed. It was shown that these elements allow an exact description of the cylinder cross-section and that they provide a powerful tool to study the effects of the geometrical modeling and of the interpolation schemes. Three kinds of cells were compared: the square, quadrilateral and transfinite cells in combination with three interpolations: the pulse, linear and transfinite quadratic interpolations. It was found on one hand that the quadrilateral cells ensure the stability of the method except very close to the resonance frequencies of the cylinder and on the other hand that to avoid memory problems the quadratic interpolation must be used in place of the pulse or the linear ones. It was thus shown that for the VSIE based MoM solution of the electromagnetic scattering by a dielectric cylinder, the best element of this study is a quadrilateral cell in combination with a quadratic interpolation, i.e., a subparametric element. However, if the relative permittivity of the cylinder is high, square cells can be used, making the VSIE based MoM compatible with iterative solvers optimized by the FFT algorithm.

#### APPENDIX

The transfinite interpolation formalism can be easily implemented in three dimensions thanks to the projectors formalism. If the  $(s, t, u)$  parameters  $\in \mathfrak{S} : [0, h] \times [0, h] \times [0, h]$  define a curvilinear coordinate system and if three one-dimensional projectors are defined as

$$\begin{aligned}
 P_s \phi(s, t, u) &= \sum_{m=1}^M \phi(s_m, t, u) u_m(s) \\
 P_t \phi(s, t, u) &= \sum_{n=1}^N \phi(s, t_n, u) v_n(t) \\
 P_u \phi(s, t, u) &= \sum_{l=1}^L \phi(s, t, u_l) w_l(u)
 \end{aligned} \tag{A.1}$$

where  $s_m$ ,  $t_n$  and  $u_l$  are three sets of interpolation nodes  $\in \mathfrak{S}$  and  $u_m(s)$ ,  $v_n(t)$  and  $w_l(u)$  are associated interpolation basis functions satisfying the cardinality condition, the transfinite interpolant



$\pi(s, t, u)$  of  $\phi(s, t, u)$  is given by

$$\pi(s, t, u) = (P_s \oplus P_t \oplus P_u)\phi(s, t, u) \quad (\text{A.2})$$

and the accuracy set of this projection is formed by the surfaces  $(s_m, t, u)$ ,  $(s, t_n, u)$  and  $(s, t, u_l)$ . The geometrical modeling and the interpolation process in the MoM can now be generalized to three dimensions in an obvious way.

## ACKNOWLEDGMENT

The author would like to thank Professor S. Prohoroff of the University of Brussels for reading this paper.

## REFERENCES

1. Taflove, A., *Computational Electrodynamics, The Finite-Difference Time-Domain Method*, Artech House, Boston. 1995.
2. Harrington, R. F., *Field Computation by Moment Methods*, The MacMillan Company, New York, 1968.
3. Massoudi, H. M., C. H. Durney, and M. F. Iskander, "Limitation of the cubical block model of man in calculating SAR distributions," *IEEE Trans. Microwave Theory Tech.*, Vol. 32, 746–751, Aug. 1984.
4. Richmond, J. H., "Scattering by a dielectric cylinder of arbitrary cross-section shape," *IEEE Trans. Antennas Propagat.*, Vol. 13, 334–341, May 1965.
5. Richmond, J. H., "TE-wave scattering by a dielectric cylinder of arbitrary cross-section shape," *IEEE Trans. Antennas Propagat.*, Vol. 14, 460–464, July 1966.
6. Borup, D. T., D. M. Sullivan, and O. P. Gandhi, "Comparison of the FFT conjugate gradient method and the finite-difference time-domain method for the 2-D absorption problem," *IEEE Trans. Microwave Theory Tech.*, Vol. 35, 383–395, Apr. 1987.
7. Peterson, A. F., and P. W. Klock, "An improved MFIE formulation for the TE-wave scattering from lossy, inhomogeneous dielectric cylinders," *IEEE Trans. Antennas Propagat.*, Vol. 36, 45–49, Jan. 1988.
8. Jin, J. M., J. L. Volakis, and V. V. Liepa, "A moment method solution of a volume-surface integral equation using isoparametric elements and point matching," *IEEE Trans. Microwave Theory Tech.*, Vol. 37, 1641–1645, Oct. 1989.

9. Gordon, W. J., and C. A. Hall, "Construction of curvilinear coordinate systems and applications to mesh generation," *Int. J. for Num. Meth. in Eng.*, Vol. 7, 461–477, 1973.
10. Jin, J. M., V. V. Liepa, and C. T. Tai, "A volume-surface integral equation for electromagnetic scattering by inhomogeneous cylinders," *JEWA*, Vol. 2, 573–588, 1988.
11. Zienkiewicz, O. C. and R. L. Taylor, *The Finite Element Method*, McGraw-Hill, London, 1994.
12. Cavendish, J. C., W. J. Gordon, and C. A. Hall, "Ritz-Galerkin approximation in blending function spaces," *Numer. Math.*, Vol. 26, 155–178, 1976.
13. De Doncker, Ph., "A transfinite moment method applied to electromagnetic scattering," *PIERS'98 Proceedings*, Vol. 2, 606, July 1998.
14. Gordon, W. J., "An operator calculus for surface and volume modeling," *IEEE Trans. CG&A*, 18–22, Oct. 1983.
15. Gan, H. and W. C. Chew, "A discrete BCG-FFT algorithm for solving 3D inhomogeneous scatterer problems," *JEWA*, Vol. 9, 1339–1357, 1995.